Technical Physics Letters, 2026, Vol. 52, No. 2

06

Semipolar aluminum nitride: the epitaxy of bulk material on a nanostructured silicon substrate

© V.N. Bessolov[1], M.E. Kompan[1], E.V. Konenkova[1], Sh.Sh. Sharofidinov[1], A.V. Solomnikova[2], M.P. Scheglov[1]

[1] Ioffe Institute, St. Petersburg, Russia
[2] St. Petersburg State Electrotechnical University „LETI“, St. Petersburg, Russia
E-mail: lena@triat.mail.ioffe.ru

Received September 16, 2025
Revised September 16, 2025
Accepted October 15, 2025

The epitaxial growth of bulk semipolar AlN layers by hydride vapour-phase epitaxy on a nanostructured silicon substrate (NP-Si(001)) was studied by X-ray diffractometry, atomic force microscopy, and Raman scattering. The semipolar layer was epitaxially grown at high growth rates in an argon atmosphere, separated from the substrate, had a thickness of $140\,\mu$m and a half-width of the X-ray diffraction curve AlN$(10\bar{1}1)$ $\omega_\theta = 60$ arcmin. It was found that the bulk semipolar AlN layer has a lower amount of stretching after removal of the substrate than the layer on the NP-Si(100) substrate.

Keywords: bulk semipolar aluminum nitride, nanostructured silicon substrate, hydride vapour-phase epitaxy

DOI: 10.61011/TPL.2026.02.63044.20500

Emitting III-N semiconductor structures are valued in optoelectronics for their small size, low power consumption, high efficiency, and extended lifetime (compared to conventional light sources). Typical emitting structure designs use InGaN/GaN chips coated with a phosphor to convert blue light into longer wavelengths. However, this process results in a loss of excitation energy, the magnitude of which is close to 25% [1]. Without the phosphor, the external quantum efficiency of LEDs operating within the yellow–green spectral range decreases [2].

Hexagonal gallium nitride (GaN) and aluminum nitride (AlN) structures feature both spontaneous and piezoelectric polarization in their lattice cell structure [3]. The polarization discontinuity at heterojunctions in heterostructures leads to the formation of layers of opposite charges at both interfaces, which induces the emergence of intense internal electric fields. The electric field reduces the overlap of electron-hole wave functions in the active region and the efficiency of radiative recombination [4]. A high fraction of indium nitride is needed to obtain green emission in the active region of structures along polar direction [0001]. However, since InGaN has a larger lattice parameter than GaN, an increase in InN fraction enhances the piezoelectric polarization effect due to structural deformation.

Studies into the growth mechanisms of aluminum nitride epitaxial layers are important for several reasons. First, hexagonal AlN is a semiconductor with a direct band gap (6.2 eV), which makes it a promising material for the production of ultraviolet optoelectronic devices. Second, thin layers of aluminum nitride are used widely as buffer layers for gallium nitride synthesis. Moreover, gallium may react chemically with Si during GaN epitaxy on silicon substrates, leading to significant degradation of the growing layer, but pre-deposition of AlN helps prevent this.

As is known, AlN grows predominantly along the AlN[0001] polar direction [5]. This leads to significant polarization perpendicular to the AlN/GaN layers, putting a limit on the quantum efficiency of emitting structures [6]. Significant research efforts have been undertaken in recent years to find ways to reduce polarization. However, no effective techniques for direct growth of non-polar or semipolar bulk aluminum nitride with a high stability of interface properties, which is required to achieve a long structure lifetime, have been proposed [7].

Only a few studies into the epitaxial growth of semipolar AlN layers on silicon substrates have been published to date. This is a rather complex technology, which was discussed in part in review [8].

The growth of semipolar AlN layers on r-sapphire, the m plane of SiC, and structured Si(100) substrates has been reported. A method for producing non-polar (cubic) gallium nitride with the use of V-shaped grooves $1\,\mu$m in width and $0.7\,\mu$m in depth, which are positioned $4\,\mu$m apart, on the Si(100) surface is known. Experiments have revealed that the growth fronts of hexagonal GaN initially form on Si faces in the process of metal-organic chemical vapor deposition (MOCVD) at low layer growth rates, but a region of cubic GaN may then arise between the growing layers [9].

In the present study, we demonstrate that the growth of AlN at high rates by hydride vapor-phase epitaxy (HVPE) on a nanostructured V-shaped Si substrate (NP-Si(100)) provides an opportunity to synthesize a structure with a semipolar AlN$(10\bar{1}1)$ plane and obtain a bulk semipolar crystalline layer separated from the substrate.

Sample fabrication is a two-step process that involves the formation of a nanostructured surface on a Si(100) substrate and subsequent HVPE growth of AlN. A series of stripes were formed first by interference lithography within a large area on the silicon substrate surface. Anisotropic etching with potassium hydroxide was then performed to obtain V-shaped grooves formed by Si$(\bar{1}11)$ and Si$(1\bar{1}1)$ surfaces adjacent at an angle of 54.7° (see the cross-sectional diagram in Fig. 1). The NP-Si(100) substrates had a faceted surface structure with periodically (45 nm) positioned crests with a height of 35 nm.

Prior to epitaxy, the substrates were treated in a 1:5 aqueous solution of hydrofluoric acid for 1 min. The growth of semipolar AlN layers with thicknesses close to $140\,\mu$m was then carried out by HVPE in argon at a temperature of $1080\,^\circ$C and rates on the order of $50\,\mu$m/h.

Two types of AlN structures were studied: those synthesized on the NP-Si(100) substrate (type A) and those obtained after substrate removal by chemical etching of silicon (type B). In X-ray measurements, rocking curves were recorded in a double-crystal diffraction arrangement in reflections (0002) and $(10\bar{1}1)$ of Cu$K_{\alpha 1}$-radiation using a triple-crystal X-ray spectrometer. The structures were studied at room temperature using atomic force microscopy (AFM) in the tapping mode with a SolverNEXT scanning probe microscope (SPM) and Raman spectroscopy with a JY HORIBA MRS 320 spectrometer.

Judging by the images of cleaved faces of the structures, the original nanostructured NP-Si(100) surface remained unchanged after epitaxy, and the layers grew in one of two possible directions: $[\bar{1}11]$ or $[1\bar{1}1]$. The results of X-ray diffraction analysis revealed that the layers had semipolar orientation $(10\bar{1}1)$ with a FWHM of X-ray diffraction curve $\omega_\theta = 60$ arcmin. It should be noted that the FWHM of X-ray diffraction for 300-nm-thick semipolar AlN $(1\bar{2}10)$ produced by MOCVD on an m-sapphire substrate was the same (approximately 3600 arcsec [10]).

The surface image in Fig. 2, a makes it evident that the AlN layer has a block nature with a block size close to $6\,\mu$m and hexagonal faceting of AlN faces. The root-mean-square (RMS) and average ((R_a)) surface roughness values for the layers were 0.805 and $0.678\,\mu$m, respectively.

SEM imaging revealed no cracks on the surface, which provided an opportunity to remove the substrate and obtain a bulk semipolar layer with a thickness of $140\,\mu$m (structure B).

The Raman spectra of AlN $(10\bar{1}1)$/NP-Si(100) for structures A and B differed (Fig. 3): peaks $E_2(high)$ ($651.2\,\mathrm{cm}^{-1}$) and A_1(TO) ($610.2\,\mathrm{cm}^{-1}$) were identified for structure A, while structure B had peaks at 652.1 and $606.7\,\mathrm{cm}^{-1}$. The spectral line associated with Si was not detected for structure B (Fig. 3). It is known that peak $E_2(high)$ for unstressed AlN is located near $657.0\,\mathrm{cm}^{-1}$ [11]. It is evident that the $E_2(high)$ line peak for AlN layers is shifted toward lower frequencies relative to its position in the non-deformed layer. This fact suggests the presence of tensile strain in the AlN$(10\bar{1}1)$/NP-Si(100) structure, and the shift magnitude is indicative of residual strain. Tensile strain in AlN$(10\bar{1}1)$ grown on NP-Si(100) is easy to explain, since the lattice parameter and the thermal expansion coefficient of AlN are smaller and larger, respectively, than those of Si. This is what leads to deformation of the structure at the epitaxy temperature and its increase upon cooling to room temperature. The Raman spectrum of the AlN layer after substrate removal reveals weaker tensile strain than that in the A-type structure.

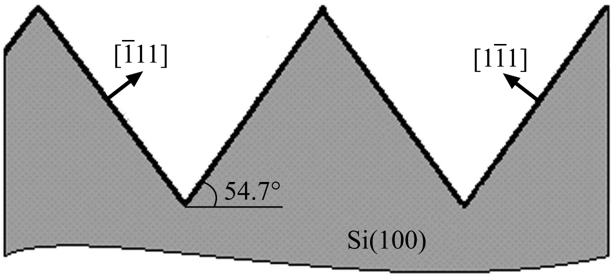

Figure 1. Schematic diagram of a groove on the NP-Si(100) surface.

The model of formation of the semipolar AlN $(10\bar{1}1)$ layer proposed here (Fig. 2, b) has two underlying elements: first, the difference in surface energy of AlN faces; second, a fairly high growth rate inherent in the HVPE method. It is known from literature that the surface energies of AlN(0001) and AlN$(000\bar{1})$ faces, which are 0.355 and $0.374\,\mathrm{eV/Å}^2$, respectively, differ. These values are significantly higher than the energy of semipolar faces (0.234 and $0.145\,\mathrm{eV/Å}^2$ for AlN$(11\bar{2}0)$ and AlN$(1\bar{1}00)$) [12]. The growth rate is known to increase with surface energy of a crystal face. The growth rate of plane (0001) should then be higher than that of plane $(11\bar{2}0)$ [13]. As is known, the layer growth regime depends on the difference in surface energies between the substrate and the formed layer during heteroepitaxy [14]. The surface energy of certain „ideal" faces of a Si crystal is known: Si(001) — $161.2\,\mathrm{meV/Å}^2$, Si(111) — $139.1\,\mathrm{meV/Å}^2$, and Si(113) — $145.8\,\mathrm{meV/Å}^2$ [15]. However, the determination of surface energies of the interfaces of semipolar AlN/Si structures is a complex task, and typical calculations of these values yield approximate values, since the influence of carrier gas in the reactor atmosphere also needs to be taken into account. For example, the surface energies of AlN faces determined in epitaxy in hydrogen or argon atmospheres differ [16]. At high layer growth rates, layers form at different rates on the Si$(\bar{1}11)$ and Si$(1\bar{1}1)$ faces of grooves, which may be attributed to the difference in concentration of defects on the surface. Notably, the highest growth rate leads to the formation of a semipolar layer in one of the two possible directions (specifically, AlN$(10\bar{1}1)$), but a significant surface roughness $R_a = 0.678\,\mu$m (Fig. 2, b) emerges at the same time.

The relatively small change of the $E_2(high)$ maximum after substrate removal is apparently indicative of a change in thermal strain in structures A and B. Indeed, growth proceeds on just one Si face in the course of epitaxy of a semipolar AlN$(10\bar{1}1)$ layer, and the second face has virtually no part in the heterostructure formation. Therefore, strain induced by the difference in thermal expansion

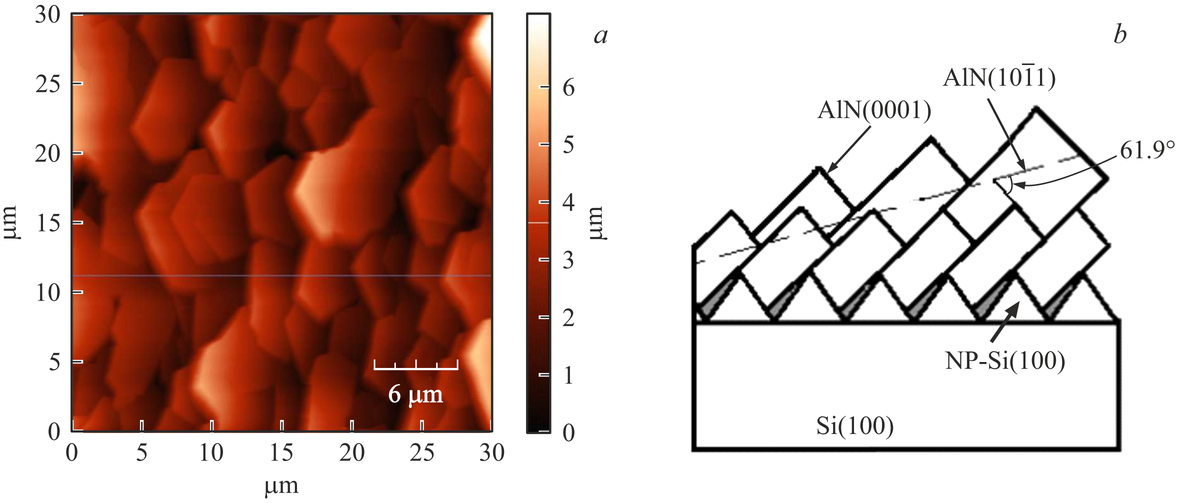

Figure 2. Surface topography of the AlN/NP-Si(100) structure with a thickness of $140\,\mu$m (*a*) and schematic diagram of the formation of AlN($10\bar{1}1$) crystals (*b*).

coefficients of Si and AlN is present in the structures, but decreases after the substrate removal due to the presence of voids on one half of the NP-Si(100) substrate (Fig. 2, *b*), and strain associated with the difference in lattice parameters of AlN and Si should produce the same contributions to the energy position of peaks for structures *A* and *B* (curves *1* and *2* in Fig. 3) at the epitaxy temperature due to the formation of defects.

Thus, a new approach to the synthesis of bulk semipolar AlN($10\bar{1}1$) with the use of high-rate layer growth by HVPE on a nanostructured silicon substrate was demonstrated. The semipolar layer was separated from the substrate and had a thickness of $140\,\mu$m and a FWHM of X-ray diffraction curve $\omega_\theta = 60$ arcmin. Raman studies revealed that the AlN layer after substrate removal had a weaker tensile strain than the AlN($10\bar{1}1$) layer obtained on NP-Si(100). Bulk AlN($10\bar{1}1$) holds promise for the production of semipolar structures based on GaN and AlGaN compounds.

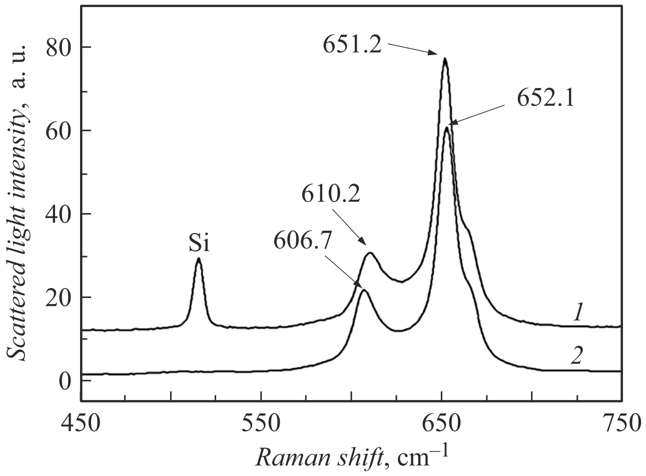

Figure 3. Raman spectra of AlN structures. *1* — Type *A*; *2* — type *B*.

Acknowledgments

The authors wish to thank the Scanning Microscopy Center of St. Petersburg Electrotechnical University „LETI“ and OOO Aktivnaya Fotonika for performing the AFM measurements.

Funding

Sh.Sh. Sharofidinov expresses his gratitude to the Russian Science Foundation for financial support (project No. 24-22-00392).

Conflict of interest

The authors declare that they have no conflict of interest.

References

[1] M. Usman, M. Munsif, U. Mushtaq, A.-R. Anwar, N. Muhammad, Crit. Rev. Solid State Mater. Sci., **46**, 450 (2021). DOI: 10.1080/10408436.2020.1819199
[2] M.H. Crawford, IEEE J. Sel. Top. Quantum Electron., **15**, 1028 (2009). DOI: 10.1109/JSTQE.2009/2013476
[3] F. Bernardini, V. Fiorentini, D. Vanderbilt, Phys. Rev. B, **56**, R10024 (1997). DOI: 10.1103/PhysRevB.56.R10024
[4] T. Takeuchi, S. Sota, M. Katsuragawa, M. Komori, H. Takeuchi, H.A.H. Amano, I.A.I. Akasaki, Jpn. J. Appl. Phys., **36**, L382 (1997). DOI: 10.1143/JJAP.36.L382
[5] S.W. King, R.J. Nemanich, R.F. Davis, J. Appl. Phys., **118**, 045304 (2015). DOI: 10.1063/1.4927515
[6] N. Sawaki, T. Hikosaka, N. Koide, Sh. Tanaka, Y. Honda, M. Yamaguchi, J. Cryst. Growth, **311**, 2867 (2009). DOI: 10.1016/j.jcrysgro.2009.01.032
[7] J.L. Li, Y.F. Li, Z.P. Liu, Nat. Commun., **16**, 4303 (2025). DOI: 10.1038/s41467-025-59613-5

[8] V.N. Bessolov, E.V. Konenkova, Tech. Phys., **68** (9), 1145 (2023). DOI: 10.61011/TP.2023.09.57354.31-23.

[9] D.M. Waters, B. Thompson, G. Ferenczi, B. Hourahine, G. Cios, A. Winkelmann, Ch.J.M. Stark, Ch. Wetzel, C. Trager-Cowan, J. Bruckbauer, J. Appl. Phys., **137**, 045701 (2025). DOI: 10.1063/5.0244438

[10] M. Jo, N. Morishita, N. Okada, Y. Itokazu, N. Kamata, K. Tadatomo, H. Hirayama, AIP Adv., **8**, 105312 (2018). DOI: 10.1063/1.5052294

[11] W. Zheng, R. Zheng, F. Huang, H. Wu, F. Li, Photon. Res., **3** (2), 38 (2015). DOI: 10.1364/prj.3.000038

[12] D. Holec, P.H. Mayrhofer, Scripta Mater., **67** (9), 760 (2012). DOI: 10.1016/j.scriptamat.2012.07.027

[13] V. Jindal, F. Shahedipour-Sandvik, J. Appl. Phys., **106** (8), 083115 (2009). DOI: 10.1063/1.3253575

[14] I.V. Markov, *Crystal growth for beginners* (Scientific, Singapore, 2003). DOI: 10.1142/5172

[15] G.-H. Lu, M. Huang, M. Cuma, F. Liu, Surf. Sci., **588** (1), 61 (2005). DOI: 10.1016/j.susc.2005.05.028

[16] T. Akiyama, H. Nakane, M. Uchino, K. Nakamura, T. Ito, Phys. Status Solidi B, **255**, 1700329 (2018). DOI: 10.1002/pssb.201700329

Translated by D.Safin